The Impact of Massive Stars on the Formation of Young Stellar Clusters

S. T. Megeath, B. Biller, T. M. Dame, E. Leass, & R. S. Whitaker

Harvard–Smithsonian Center for Astrophysics, 60 Garden St, Cambridge, MA 02138, USA

T. L. Wilson

SMTO, Steward Observatory, University of Arizona, Tucson, AZ 85721, USA & MPIfR, Postfach 2024, D-53010, Bonn, Germany

Abstract.
Massive OB stars play an important role in the evolution of molecular clouds and star forming regions. The OB stars both photo–ionize molecular gas as well as sweep up and compress interstellar gas through winds, ionization fronts, and supernovae. In this contribution, we examine the effect massive stars have on the formation of young stellar clusters. We first discuss the processes by which OB stars destroy cluster–forming molecular cores, and hence terminate star formation. We overview observational evidence that OB stars forming in young stellar clusters destroy their parental cores on a timescale of 0.1 Myr, and we discuss some of the implications of this result. We then summarize extensive observations of the NGC 281 molecular cloud complex, and present evidence that two types of triggered star formation are occurring in this complex. Our goal is to underscore the impact massive stars have on cluster formation over distances ranging from 0.1 pc to 300 pc.

1. Introduction

Stars are formed not in isolation, but in associations, groups and clusters. Associations span tens of parsecs and are defined by the molecular cloud complexes from which their constituent stars form; some examples are the T association in the Taurus molecular cloud, and the extensive association of OB stars interacting with the Orion molecular clouds. Within these molecular clouds, star formation is typically not widespread, but concentrated into distinct, parsec–sized groups and clusters with memberships ranging from ten stars to a thousand stars[1]. The stars in associations and clusters are not formed simultaneously in a single star forming event, but over a span of 1 Myr in clusters (Palla & Stahler 2000), and a span of several to 10 Myr in associations (Briceño et al. 2001). The immediate

---

[1]Since systems of more than 100 young stars may persist as gravitationally bound open clusters, Adam & Myers (2001) define clusters as systems of more than 100 stars, and groups as systems containing less than 100 stars.

implication of both the non-isolated and non-coeval nature of star formation is that the formation of stars can be affected by winds, radiation, and outflows from previous generations of stars.

OB stars have the most dramatic influence on star formation. These stars both ionize and photodissociate molecular clouds with their intense UV radiation and sweep up atomic and molecular gas with winds, ionization fronts, and – at the end of their lives – supernovae. In particular, stars with spectral types of B2 or earlier produce enough UV radiation to effectively ionize cluster–forming molecular cores. Since OB stars are relatively rare, it is important to assess their importance by examining unbiased near–IR surveys of molecular clouds. In an analysis of the 2MASS 2nd incremental release data covering the Perseus, MonR2, Orion A and Orion B clouds, Carpenter (2000) found a total of 1200 isolated stars, 200 stars in eight groups, and 2900 stars in six clusters. Hence, the majority of the stars in these clouds formed in clusters containing 100 or more stars. In the sample, four of the clusters, GGD12-15, Mon R2, NGC 2024 & the Orion Nebula Cluster, contain at least one star with a spectral type of B2 or earlier. One of the groups, NGC 2068[2], contains a B1.5 star. In total, 57% of the stars detected in the studied regions are in close proximity to ionizing OB stars. This number is a lower limit since it only counts OB stars which form within clusters. As we will demonstrate, external OB stars may also influence the formation of clusters.

In this paper, we discuss how massive stars influence the process of cluster formation on sizescales ranging from 0.1 pc to 300 pc, with a particular emphasis on our own study of the NGC 281 region. We start by examining the disruption of cluster–forming molecular cores by nascent OB stars within the cluster. As we demonstrated above, the majority of observed young clusters appear to contain OB stars. We then study the disruption of cluster forming cores by neighboring OB stars, which are situated a few parsecs away from the star forming region. This case occurs during the formation of an OB association, when OB stars which have dispersed their own parental cores begin to ionize neighboring star forming cores. Finally, we discuss a possible case of supernova driven star formation, where the influence of OB stars extends beyond the boundaries of molecular cloud complexes to distances of a few hundred parsecs.

2.   Core Destruction by Internal OB Stars (< 1 pc)

The birth sites of massive stars are 1000 $M_\odot$ dense molecular cores with densities of 10^5 cm^{-3} and sizes of 1 pc (Plume et al. 1997). Within these cores, entire clusters of lower–mass stars form. OB stars still embedded within their parental cores are thought to form ultracompact HII regions (UCHIIs), HII regions with sizes of < 0.1 pc and electron densities $> 10^4$ cm^{-3}. This picture is supported by the growing number of observations showing UCHIIs surrounded by embedded clusters of lower–mass stars (Megeath et al. 1996; Tapia, Persi & Roth 1996;

---

[2]Our classification of NGC 2068 as a group is due to the partial coverage of this region in the 2nd incremental release of the 2MASS data. While Carpenter finds only 45 stars in the incomplete 2MASS data, Lada (1989) reports 192 stars in the region, indicating that NGC 2068 should be classified as a cluster.
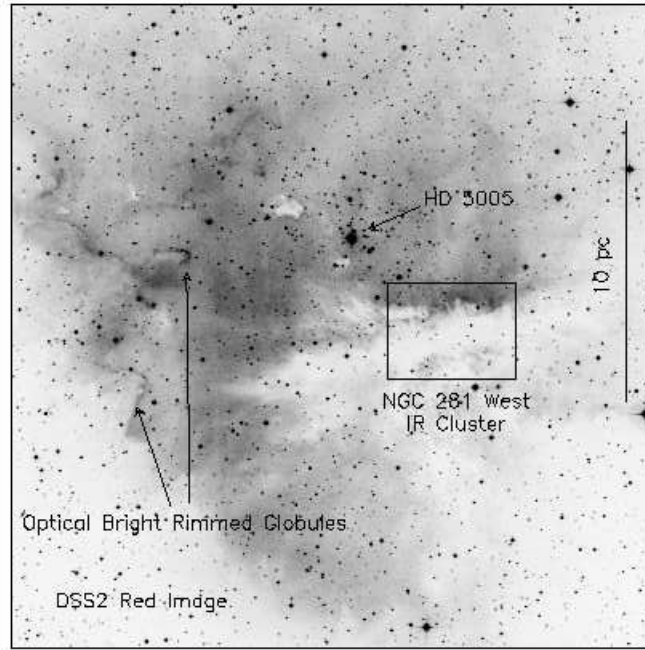
Figure 1.   2nd Generation Digital Sky Survey, red band image of the NGC 281 Nebula and IC 1590 Cluster. The primary ionizing star is HD 5005, an O5.5 star. The eastern side of the nebula shows numerous bright rimmed globules, but the most active region of ongoing star formation is the obscured IR cluster towards the southwestern quadrant of the nebula.

Pratap, Megeath & Bergin 1999). After OB stars dissipate their parental dense cores, the HII regions expand and are no longer classified as UCHIIs (Tieftrunk et al. 1997). Hence, the lifetime of UCHIIs is the time required for young OB stars, once they have formed, to destroy their parental cores and terminate the process of cluster formation.

The best current estimates of the lifetimes of UCHIIs are based on empirical arguments. Wood & Churchwell (1989) found that UCHIIs can be identified on the basis of their IRAS colors. By comparing the number of IRAS identified UCHIIs in the Galaxy with the observed number of OB stars in the solar neighborhood, they estimated a lifetime of 0.5 Myr. By eliminating lower–mass stars contaminating the IRAS sample, as well as taking into account variations in the density of UCHIIs with galactic radius, this lifetime has been revised by Comeron & Torra (1996) and Casassus et al. (2000) to $0.05 - 0.1$ Myr.

The estimated UCHII lifetimes indicate that once an OB star is formed in a cluster forming core, the core destruction occurs on a timescale of 0.1 Myr. Since the timescale for cluster formation is ten times longer, 1 Myr (Palla & Stahler 2000), only 1/10 of the forming clusters should contain ultracompact HII regions. Interestingly, in the combined surveys of W3 (Tieftrunk et al. 1998), Perseus, Orion A, Mon R2 (Carpenter 2000) & Orion B (Lada 1992), 4/10 of the clusters contain UCHIIs: Mon R2, W3 OH, W3 Main, and GGD12-15. Although the
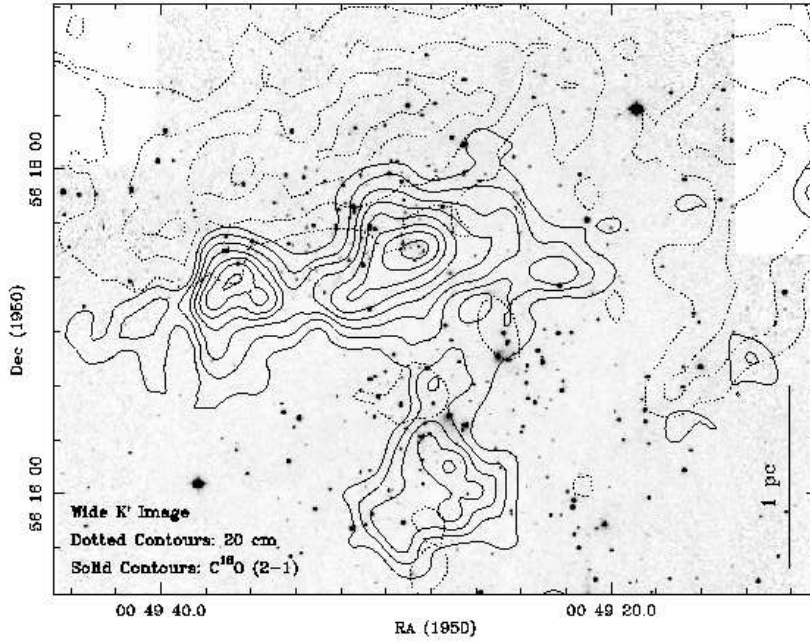
Figure 2. Greyscale: 2 μm image of the NGC 281 West cluster. Dotted contours: 20 cm VLA data tracing the ionized gas. The contour levels are 1.8 to 5.4 by 1.8 mJy/beam. Solid contours: $C^{18}O$ ($2 \rightarrow 1$) IRAM 30 m map of the molecular gas in the interface. The contours levels are 5.24 to 15.72 by 1.747 K km s^{-1}. The ionizing star, HD5005, is 4 pc to the northeast of the molecular cores (outside the near–IR image). Note that the cluster is divided into northern and southern sub-cluster.

ratio is four times that expected, the current sample of molecular clouds is small. A larger sample is needed to firmly establish the fraction of star–forming clusters with UCHIIs.

3. Core Destruction by External OB Stars (1-10 pc)

Optical images of HII regions commonly show bright rimmed and cometary globules: dense molecular gas that survives in the HII region once the surrounding, lower density gas is swept away. These globules are directly exposed to the UV radiation from OB stars within the HII region. In a process called photoevaporation, the UV radiation produces a flow of ionized gas off the surfaces of the clump; the optical line emission producing the bright rims arises in this ionized flow. Despite the continual erosion of the molecular gas, a theoretical analysis by Bertoldi & McKee (1990) has demonstrated that these globules can survive for millions of years in the HII region, depending on their mass and distance from the OB stars. This relatively long timescale for the core destruction allows for the formation of groups and clusters in the exposed cores. Several examples
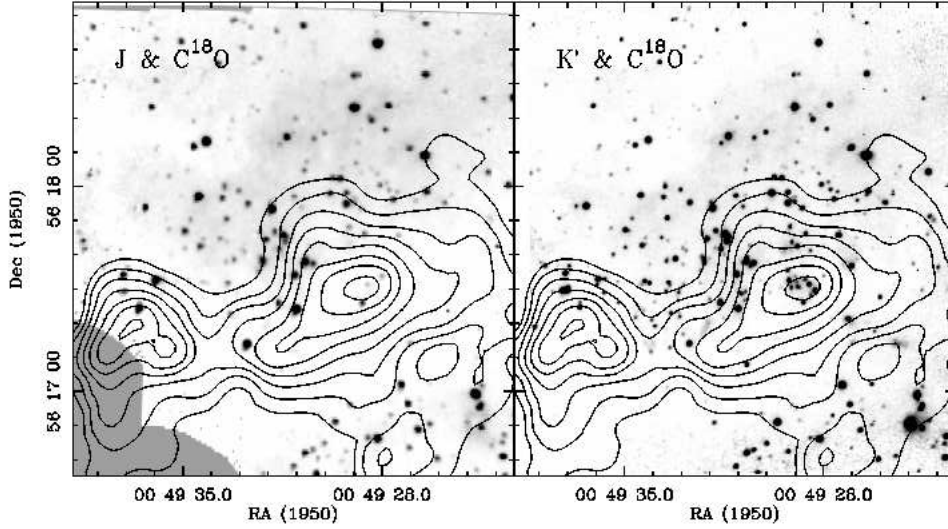
Figure 3. Left: J-band image of the NGC 281 HII/H$_2$ interface with contours of the C^{18}O (2 → 1) emission overlaid. Right: K-band image with C^{18}O contours. The images are centered on the northern subcluster, which is associated with the two northernmost molecular cores. The stars apparent in the bottom right corner of the images are in the southern sub-cluster associated with the southernmost molecular core (see Fig. 2).

of young stellar groups forming in bright rimmed globules have been reported by Sugitani, Tamura & Ogura (1995).

The formation of groups and clusters in externally ionized cores may not result solely from the long destruction timescales, but also from the triggering of star formation by the ionization. A likely example of triggered cluster formation is the NGC 281 infrared cluster, the richest cluster yet observed towards a bright rimmed globule. It is the most active region of ongoing star formation in NGC 281, containing at least one massive star, as evidenced by a 10^4 L$_\odot$ IRAS source (Henning 1994), and a cluster of 240 lower–mass stars, as detected in near–IR images (Megeath & Wilson 1997). The infrared cluster, located in the southwestern quadrant of the NGC 281 nebula, is not associated with the optical bright rimmed globules apparent in the nebula (Fig. 1).

The evidence for triggered star formation comes from combined centimeter, millimeter, and near–IR data. Since optical observations of this region are complicated by a spatially varying extinction, we obtained C^{18}O maps, tracing the dense cores, and a VLA 20 cm map, tracing the ionized gas, to disentangle the structure of the H$_2$/HII interface with angular resolutions $< 20''$. The maps show that the molecular gas is concentrated into three main cores and several smaller clumps (Fig. 2). To the northern edges of each core, 20 cm emission tracing the ionized gas is detected, with particularly strong 20 cm emission adjacent to the two northernmost cores. These cores are *radio* bright rimmed globules. In support of the radio data, recent Hubble space telescopes images taken with the WFPC2 camera show the optical emission from Hα and [SII] lines extending
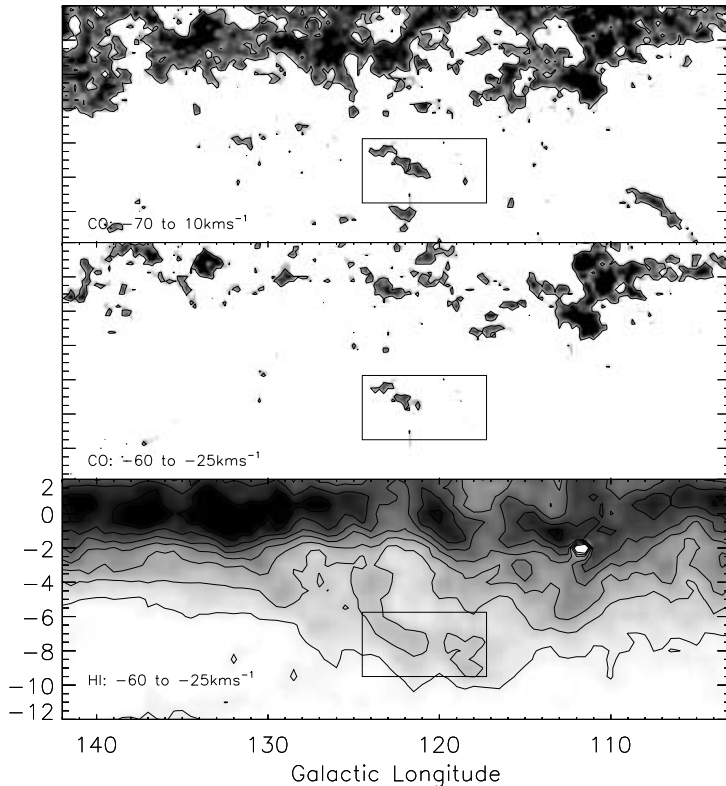
Figure 4.   The velocity–integrated CO $(1 \rightarrow 0)$ line emission and HI 21 cm line emission from the CfA CO survey and the Leiden–Dwingeloo HI survey (Dame, Hartmann & Thaddeus 2001; Hartmann & Burton 1997). Top: the local and Perseus arm velocity gas. Middle: The Perseus arm velocity gas. Bottom: 21 cm map of the HI emission integrated over the Perseus arm velocities. The NGC 281 cloud complex is delimited by the rectangle.

to the cores. These data demonstrate that the cores are exposed to the UV radiation from the ionizing O star, and are photoevaporating. Megeath & Wilson (1997) estimate that at the current rate of photoevaporation, the observed cores will be fully evaporated in 2.5 Myr.

A comparison of the pressure from the ionized, photoevaporating gas at the clump surfaces to the turbulent pressure of the molecular gas in the clumps, indicates that the pressure of the ionized gas is sufficient to drive shock waves into the molecular cores. The shocks would have a velocity of 1.5 km s^{-1} and a crossing time of 0.7 Myr. The C^{18}O data show a ridge of blueshifted gas along the northern edge of the cores: this may be the detection of gas swept up by the shock (see Megeath & Wilson 1997).

Near–IR images of the two northermost cores show a steep gradient in the surface density of stars with most of the embedded stars concentrated near the photoevaporating surfaces of the cores (Fig. 3). The lack of a corresponding gradient in the extinction through the cores, as demonstrated by the C^{18}O maps, implies that the observed gradient in stellar density is due to an asymmetric

distribution of stars. Megeath & Wilson (1997) have proposed that the asymmetry is the result of triggered star formation. In this picture, the shock fronts have traversed roughly halfway through the cores. As the shocks compress the gas, they precipitate the formation of stars which then fill the post-shock gas. Near–IR imaging of groups in optical bright rimmed globules have detected similar asymmetries in the distribution of stars (Sugitani, Tamura & Ogura 1995). These data suggest that shock–triggered formation may be a common process in cores exposed to the UV radiation from neighboring OB stars.

4.   Supernovae Driven Formation of Clusters (> 100 pc)

The NGC 281 nebula is part of a complex of molecular clouds in the Perseus arm of the galaxy (Fig. 4). The measured distance to the nebula (2.9 kpc; Guetter & Turner 1997) implies that the complex is located 300 pc below the galactic plane; in contrast, the rest of the Perseus arm clouds are found within 150 pc of the plane. Another unusual property of the NGC 281 complex is the high dispersion in cloud velocities: the longitude-velocity diagram in Fig. 5 shows a dispersion of 45 km s^{-1}. The high velocity dispersion suggests that the complex may only be a chance alignment of clouds in the sky. However, the lack of other Perseus arm clouds at these galactic latitudes, the linking of the CO clouds by the HI emission (Fig. 4 and 5), and the elliptical distribution of CO and HI emission in the longitude-velocity diagram, all support the notion that these clouds form a bona fide complex of molecular and atomic clouds.

The elliptical pattern evident in the longitude-velocity diagram is indicative of an expanding ring. The diameter of the ring is 270 pc, the expansion velocity in the line of sight is 22 km s^{-1}, and the resulting dynamical time is 6 Myr. The mass in molecular gas, using a standard conversion from the velocity–integrated CO temperatures to H_2 column density, is 10^5 M$_\odot$. The HI mass integrated over latitudes of -6° to -11° and velocities of -15 km s^{-1} to -60 km s^{-1} is 3.5×10^5 M$_\odot$. The resulting kinetic energy is 4.5×10^{51} ergs, comparable to the energy of a supernova.

We are currently exploring the possibility that the ring has formed in gas lifted out of the plane by the expansion of a superbubble. The HI emission in the NGC 281 complex forms part of a loop of HI extending out of the plane; this loop may trace the shell of a superbubble driven by supernovae and winds from OB associations near the plane of the Galaxy (Fig. 4). Models of superbubbles expanding into a stratified galactic "atmosphere" predict that at a distance of a few hundred parsecs above the plane, the upward expansion of the bubble accelerates resulting in a blowout (MacLow & McCray 1988). Numerical simulations of blowouts predict that the fragmenting shell can have velocities as large as 50 km s^{-1} *tangential* to the galactic plane (MacLow, McCray & Norman 1989). It is then plausible that the observed expanding ring has been formed in a blowout, with the clouds located at the distance from the plane where the blowout started. This interpretation suggests that the formation of the entire NGC 281 complex has been triggered by previous generations of OB stars. This mode would operate on a totally different timescale (6 Myr vs 1 Myr) and sizescale (300 pc vs 4 pc) than the triggered star formation discussed in the previous section.
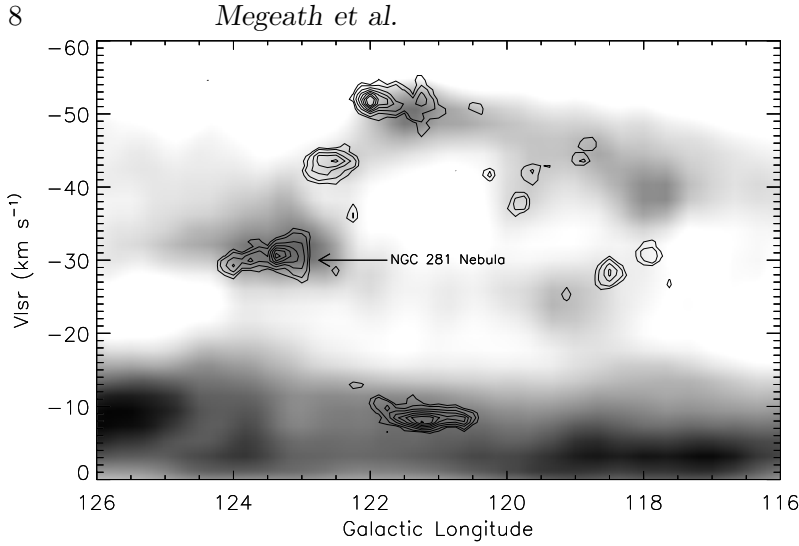
Figure 5.   Longitude-velocity diagram of the CO $(1 \rightarrow 0)$ (contours) and HI 21 cm emission (greyscale) integrated over $b = -8^o$ to -5°. The contours levels are 0.1, 0.2 to 1.4 by 0.2 K deg.

References

Bertoldi, F. & McKee, C. F. 1990 ApJ 354, 529.

Briceño, C., Vivas, A. K., Calvet, N. et al. 2001 Sci, 291, 93.

Carpenter, J. M. 2000 AJ 120, 3139.

Casassus, S., Bronfman, L, & May, J. et al. 2000 A&A 358, 514.

Comeron, F. & Torra, J. 1996, A&A 314, 776.

Dame, T. M., Hartmann, D., & Thaddeus, P. 2001 ApJ 547, 792.

Guetter, H. H. & Turner, D. G. 1997 AJ 113, 2116.

Hartmann, D. & Burton, W. B. 1997, Atlas of Galactic Neutral Hydrogen (Cambridge: Cambridge Univ. Press).

Henning, Th., Martin, K., Reimann, H.-G., et al. 1994 A&A 288, 282.

Lada, E. A. 1992 ApJ 393, L25.

MacLow, M.-M., McCray, R. 1988 ApJ 324, 776.

MacLow, M.-M., McCray, R. & Norman, M. L. 1989 ApJ 337, 141.

Megeath, S. T., Herter, T., Beichman, C., et al. 1996 A&A 307, 775.

Megeath & Wilson 1997 AJ 114, 1106.

Palla, F., Stahler, S. W. 2000 ApJ 540, 255.

Plume, R., Jaffe, D. T., Evans, N. J., II. et al. 1997, ApJ 476, 730.

Pratap, P., Megeath, S. T., & Bergin, E. A. 1999 ApJ 517, 799.

Sugitani, K., Tamura, M., & Ogura, K. 1995 ApJ 455, L31.

Tapia M., Persi, P., & Roth, M. 1996 A&A 316, 102.

Tieftrunk, A. R., Megeath, S. T., Wilson, T. L., et al. 1998 A&A 336, 991.

Tieftrunk, A. R., Gaume, R. A., Claussen, M. J., et al. 1997 A&A 318, 931.

Wood, D. O. S. & Churchwell, E. 1989 ApJ 340, 265.